Int J Thermophys (2008) 29:1578–1588
DOI 10.1007/s10765-008-0462-5

The New KRISS Low Frost-Point Humidity Generator

B. I. Choi · H. S. Nham · S. B. Woo · J. C. Kim · S. Y. Kwon

Published online: 5 June 2008

Abstract A new low frost-point humidity generator (LFPG) has been designed, and its performance has been tested, in order to extend the calibration capabilities to the low frost-point range at KRISS. The water vapor–gas mixture is generated by saturating air with water vapor over a surface of an ice-coated saturator under the conditions of constant temperature and pressure. This LFPG covers a range of frost point from −99 °C to −40 °C. The temperature of the saturator, which is controlled by thermoelectric devices and a two-stage mechanical refrigeration system, is stable within 5 mK, and the difference between the saturator temperature and the frost point generated at the saturator outlet is less than 20 mK. This stability is achieved by using oxygen-free high-conductivity copper materials as the saturator body, and applying a precision PID temperature control system. The performance of this new LFPG system is compared with the KRISS standard two-temperature generator in the frost-point range (−80 to −40) °C, and its performance is tested with a quartz crystal microbalance (QCM), which was built at KRISS, to −91 °C.

Keywords Dew point · Frost point · Humidity standard · Low frost-point generator · Quartz crystal microbalance · Thermoelectric device

1 Introduction

The main activities of the Korea Research Institute of Standards and Science (KRISS) in the field of humidity are focused on the maintenance and improvement of primary standards. In addition, KRISS provides humidity calibration services, to enable accurate and uniform humidity measurements throughout Korea and abroad. In most

B. I. Choi (✉) · H. S. Nham · S. B. Woo · J. C. Kim · S. Y. Kwon
Division of Physical Metrology, Korea Research Institute of Standards and Science,
1 Doryong-Dong Yuseong-Gu, Daejeon 305-340, Korea
e-mail: cbi@kriss.re.kr

national standard laboratories, precision humidity generators based on the saturation of water vapor have been used as the primary humidity standard. The KRISS has already two primary humidity generators, and has been disseminating a dew-point standard between −70 °C and +25 °C through its accredited calibration service. Our first precision humidity generator, based on the two-pressure two-temperature (2T2P) principle and operating in the dew-point range from −10 °C to +25 °C, was established in the early 1990s. A few years later, the second two-temperature (2T) generator was constructed, extending the calibration range to a frost point of −70 °C.

However, its lowest achievable water vapor corresponds to ppm levels in mole fraction, which is far greater than the ppb level of moisture required in modern industries. As new technologies have emerged, more accurate measurement and control of the mole fraction of water vapor (10 nmol · mol^{-1} and lower) is required in various fields, such as the semiconductor and microelectronic manufacturing process. To respond to this demand, KRISS has constructed and evaluated a new low frost-point humidity generator (LFPG), which is similar to the one at NIST [1–3], in order to extend the range of the humidity standard to the ppb level. This LFPG operates from −99 °C to −40 °C in the frost-point range, which spans four decades in mole fraction of water vapor, covering the range 18 nmol · mol^{-1} to 130 μmol · mol^{-1}.

2 Low Frost-Point Generator

Currently, most types of humidity generators for reference purposes are saturator-based, which operate by saturating the air inside the saturator at a specific temperature and pressure, and then taking it to a measuring chamber at a different temperature and/or pressure, to produce air with the desired level of humidity. There are two-pressure generators, two-temperature generators, and combined two-pressure and two-temperature generators. A key difference between two-pressure and two-temperature generators is that, in a two-pressure generator, a gas stream is saturated with water vapor at an elevated pressure with subsequent gas expansion in order to produce different dew/frost points from a single saturator temperature; in a two-temperature generator, a gas stream is saturated with water vapor at a gas pressure, nominally the hygrometer inlet pressure, with no significant gas expansion. In this case, different dew/frost points are generated by changing the saturator temperature.

The dew/frost point of the generator can be expressed as follows:

$$f(T_\mathrm{d}, P_\mathrm{t}) \times e_\mathrm{s}(T_\mathrm{d}) = f(T_\mathrm{s}, P_\mathrm{s}) \times e_\mathrm{s}(T_\mathrm{s}) \times \frac{P_\mathrm{t}}{P_\mathrm{s}} \tag{1}$$

where T_s = temperature in the saturator; T_t = temperature in the test chamber or in the hygrometer; P_s = pressure in the saturator; P_t = pressure in the test chamber or in the hygrometer; $e(T)$ = water vapor pressure at T [4]; and $f(T, P)$ = enhancement factor at T, P [5].

In a two-temperature generator, P_s is equal to P_t. In this study, a two-temperature type generator is chosen primarily because its humid air flow is relatively simple since there is no need to have an expansion valve to reduce the air pressure (as in

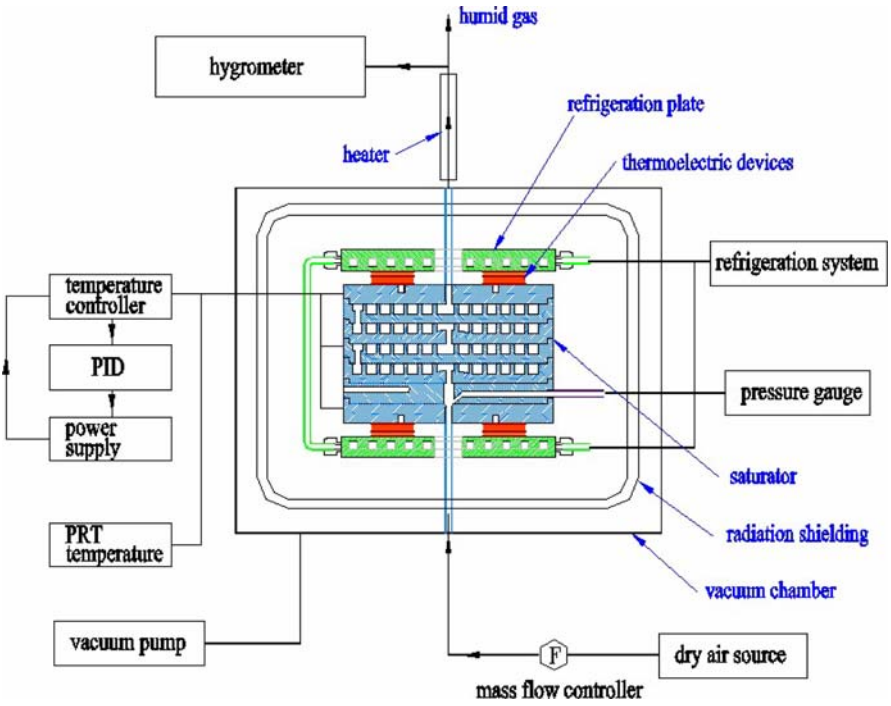

Fig. 1 Schematic diagram of the low frost-point generator

a two-pressure generator), although it has many other advantages. In the low frost-point region, the water vapor density is extremely low (at a frost point of −90 °C, $7 \times 10^{-5}\,\mathrm{g \cdot m^{-3}}$), and it is important to keep the gas flow as simple as possible for the stable control of the humid gas. Another reason for this choice is that the uncertainty resulting from the enhancement factor can be reduced, largely because the pressure used is close to atmospheric pressure.

An overall schematic for the constructed low frost-point generator (LFPG) is shown in Fig. 1. The gas introduced to the LFPG is nitrogen evaporated from liquid nitrogen with a frost point below −90 °C. If the frost point of the initial gas is relatively high and used over a long period of time, the gas-flow path could become blocked due to the formation of ice in the saturator. The flow is controlled by a mass-flow controller (MFC) to a preset value of 1 liter per minute, and gas is humidified in the saturator before exiting via an electro-polished stainless-steel tube. This tube is wound with a heater wire from the vacuum chamber outlet port to the hygrometer, allowing its temperature to be elevated up to 100 °C. The heater can be used to evaporate and remove the moisture remaining inside the tube in the event that there is an ultra-low frost point (<–90 °C).

Humid gas generation is of the frost-point type, which uses quasi-equilibrium states inside the saturator and slowly moisturizes the passing gas with the evaporated and saturated water vapor rising from the surface of the ice. This process involves the natural

vapor pressure from a condensed substance (a function of temperature), which allows us to interpret the results analytically, and provides us with stable measurements.

The system consists of the saturator, gas purifier, refrigeration system, thermoelectric cooling device, vacuum chamber, gas tubing, flow controller, and measuring instruments for temperature and pressure. In Fig. 2, core parts such as the saturator in the vacuum chamber, the cooling stage, the thermoelectric cooling device, and the temperature sensors are shown. The material used for the saturator is OFHC (oxygen-free, high-conductivity copper), a material with high thermal conductivity, which aids the stability and uniformity of temperature. There were difficulties in the fabrication of the saturator, such as machining, surface finishing of the inside of the saturator, and brazing techniques for the whole assembly, but it was built and, after some trial and error, was eventually found to be working well. The structure inside the saturator should be built in such a way that proper gas flow over the surface of either ice or water is allowed, in order for mass exchange to occur smoothly between the surface and the gas above. The flow pattern in this case should be turbulent to maximize the mass exchange. The path for the gas flow inside the saturator is a channel 9.5 mm deep and 9.3 mm wide that was machined by milling in the shape of a spiral 7 m long before connecting to the next stage, which is long enough to have effective mass exchange for full saturation. This channel is filled to half its capacity with water and frozen slowly, to be used as the water vapor source. In total, the saturator consists of four blocks with a machined path for saturation, one block with ports for monitoring the temperature and pressure, and two blocks for the inlet and outlet of the gas, and all of them are vacuum brazed. The inner surfaces of the water channels are electroplated with nickel

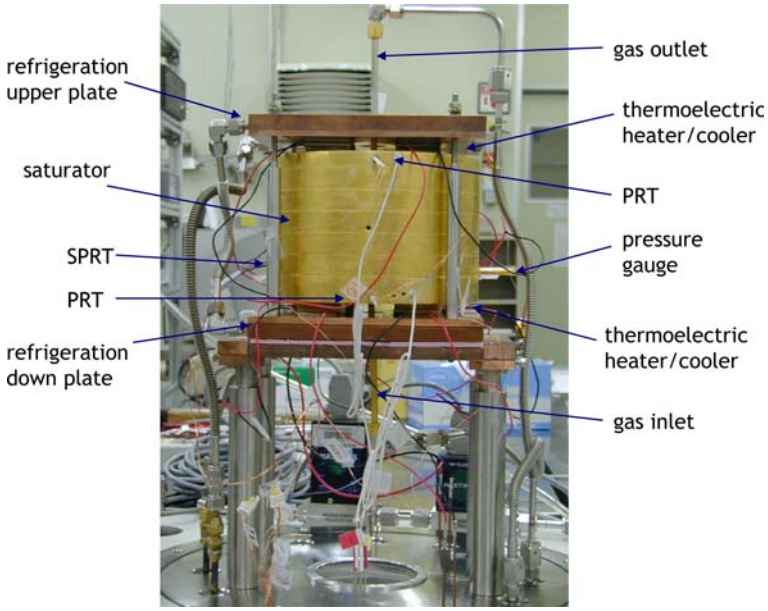

Fig. 2 Inside view of the low frost-point generator system

to prevent oxidation, and were completely washed before being vacuum brazed. The outer surface is gold-coated to improve thermal conduction.

What is important in a good LFPG is the cooling capacity for the entire saturator system, which must establish precise temperature control and maintain temperature stability over long periods of time. The cooling is done by a two-stage mechanical refrigerator with ethylene gas as the cooling medium, and it is able to cool the cold plate down to a low enough temperature to produce $-99\,^{\circ}\mathrm{C}$ frost point gas. Temperature control of the saturator is achieved through eight thermoelectric-cooling devices placed between the upper and lower cold plates and the saturator. Four thermoelectric-cooling devices in each pair of top and bottom sides are located near the middle of the top and bottom faces of the saturator, for symmetrical thermal conduction, and are oriented toward the center at each device's location. For maximum thermal conduction between the thermoelectric-cooling devices, the saturator, and the cooling plates, the flatness and smoothness of each contacting surface must be assured, and a high-thermal-conductivity paste is applied. The temperature control of the thermoelectric-cooling device is done through PID control, with the top and bottom plates controlled by two separate controllers. The temperature sensors for the control are two platinum resistance thermometers (PRTs), one placed on the top block and the other on the bottom block. The saturator temperature is determined from the standard platinum resistance thermometer (SPRT) (Hart Scientific Model 5686) inserted into the saturator. Two more PRTs are attached to the ends of the top and bottom of the saturator to monitor the temperature gradient.

To minimize thermal radiation and conduction from the saturator to the outside environment and to achieve good temperature stabilization, the whole system is covered with three layers of thin Mylar film, and is placed inside a vacuum chamber (usually $<10^{-7}$ Torr). To support the saturator and cooling plate, thin-walled (0.1 mm) stainless-steel tubes are used, and the electrical leads to the temperature sensors are thermally anchored to the intermediate-temperature reservoir before they are connected to posts at room temperature. The inlet and outlet tubes for the gas are located in the center of the saturator, so that thermal flux entering the system is symmetrically distributed.

3 Performance Test

3.1 Temperature Stability

Maintaining good temperature stability in the saturator is a very important factor in the performance of an LFPG. The saturator temperature is controlled by two thermoelectric-cooling device controllers, with the respective temperature sensors located on the top and bottom blocks of the saturator. Covering the saturator with thin Mylar films to minimize the outside thermal influence was of great help in ensuring temperature stability. The temperature stability of the saturator can be influenced by the resolution of the temperature sensor, fluctuation in the refrigerator, and the ability of the PID control. Figure 3 shows the temperature stability measured at a temperature around

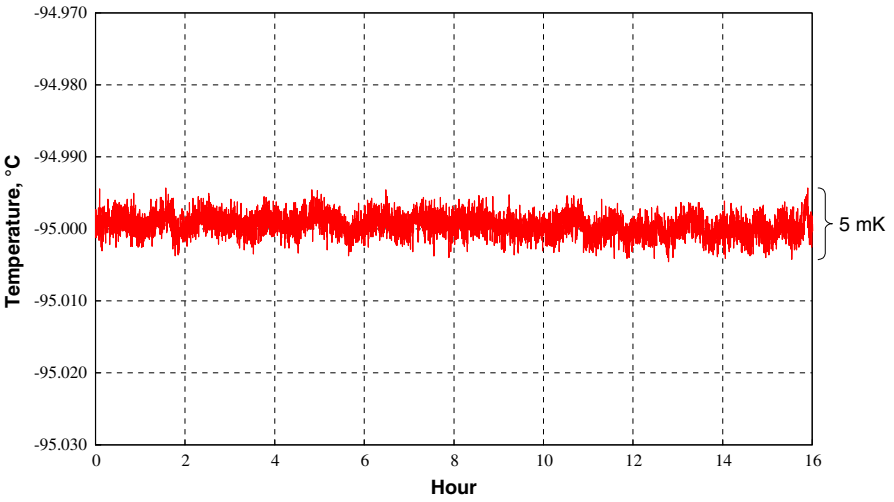

Fig. 3 Temperature stability of saturator in the LFPG

−95 °C, where the temperature was stable within 5 mK for over 16 h. A stability of 5 mK can also be seen at other temperatures.

The temperature gradient is monitored by the PRT sensors located at both ends of the saturator, but the measured values from these sensors are not particularly helpful because they are not calibrated. Instead, they are used to monitor the temperature behavior for extreme thermal inputs to the saturator. The extreme thermal change is made by cutting off the power to the thermoelectric cooling devices of one side of the saturator when the system has reached thermal equilibrium, while the other side is kept constant. Then, the temperature difference indicated by the PRTs is monitored. Next, the process is reversed, and the temperature difference is monitored. From this measurement, the temperature gradient of the saturator is observed to change by less than 20 mK. This result is achieved due to the high thermal conductivity of the OFHC copper that was used to construct the saturator.

3.2 Saturation Capability

Humid gas inside the saturator should contact the ice surface long enough to quickly reach and maintain thermal equilibrium, and hence become fully saturated. The constructed saturator has a gas path length of 7 m, which is long enough for full mass exchange, and should guarantee complete saturation. If the humid gas at the exit is not saturated, one has to check for the possible reasons, such as a short saturation path, an excessive gas flow, or an inappropriate inlet gas temperature. In Fig. 4, the measured frost points of the exit gas are shown when the inlet gas is changed from dry to humid and vice versa in order to evaluate the efficiency of the saturator. With the saturator temperature set to −70 °C, the frost point of dry gas is below −95 °C and the humid gas frost point is −63 °C. The gas densities of the dry and humid gas are

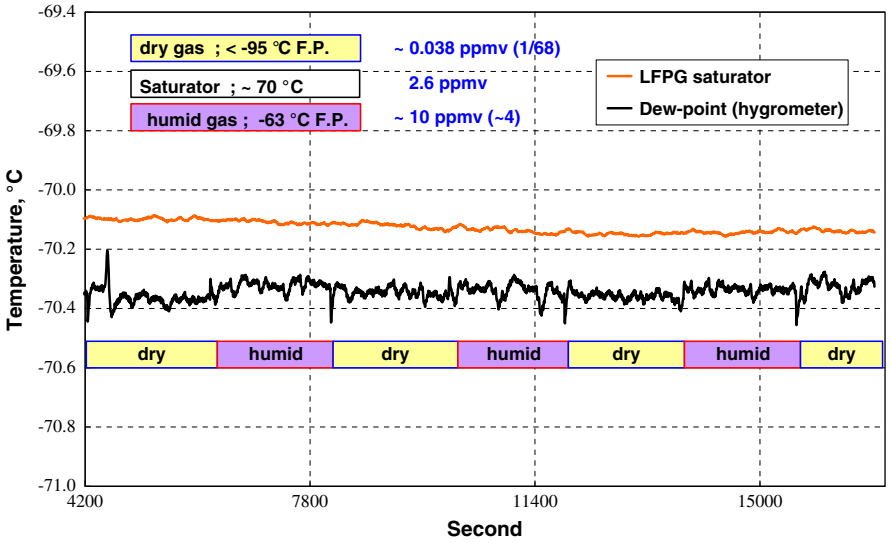

Fig. 4 Saturation capability test with dry (frost point $< -95\,°C$) and humid (frost point $-63\,°C$) gas at a saturator temperature of $-70\,°C$

1/68th ($0.038\,ppm_v$) and 4 times ($10\,ppm_v$) that of $-70\,°C$ frost-point gas ($2.6\,ppm_v$). In the event of low saturation, the measured frost point of the exit gas should be lower than $-70\,°C$ for dry inlet gas and higher for humid inlet gas. In Fig. 4, no frost-point change is observed between the two cases, and this means that the saturation capability is large enough for the purpose. Similar results can be obtained to the upper frost-point limit of $40\,°C$.

The water vapor concentration produced by a saturator of sufficient length should be both independent of the water–vapor concentration of the gas entering the saturator, and independent of the carrier gas flow rate through the saturator. The results shown in Fig. 5 support this for a saturator temperature of $-70\,°C$. Figure 5 shows the results of the saturation capability testing in terms of flow rate change from 1 to $5\,L \cdot min^{-1}$ with dry and humid gas. If the saturation capability is insufficient, the measured frost point of the exit gas should decrease as the flow rate increases when dry gas enters the saturator, and should increase when humid gas enters. However, we could not find the anticipated difference between the dry gas and the humid one. This result is further evidence that the capability of the saturator is sufficient. As shown in Fig. 5, the frost point at the hygrometer decreases by about (0.1–0.2) °C in both cases. This must be due to the temperature drop of the vapor in the gas line as the flow rate increases. The vapor temperature in the gas tube apparently changed with the gas flow rate. The temperature of the vapor measured at the outlet of the vacuum chamber dropped from $-45\,°C$ to $-61\,°C$ when the flow rate increased from 1 to $5\,L \cdot min^{-1}$, at $-70\,°C$ saturator temperature. Meanwhile, that at the hygrometer remained the same, $22\,°C$. These temperature drops of the vapor in the gas line, which lies between the saturator and the hygrometer, has changed the adsorbed amount on the wall of the gas tube, and decreased the frost point. On the other hand, the pressure drops between the

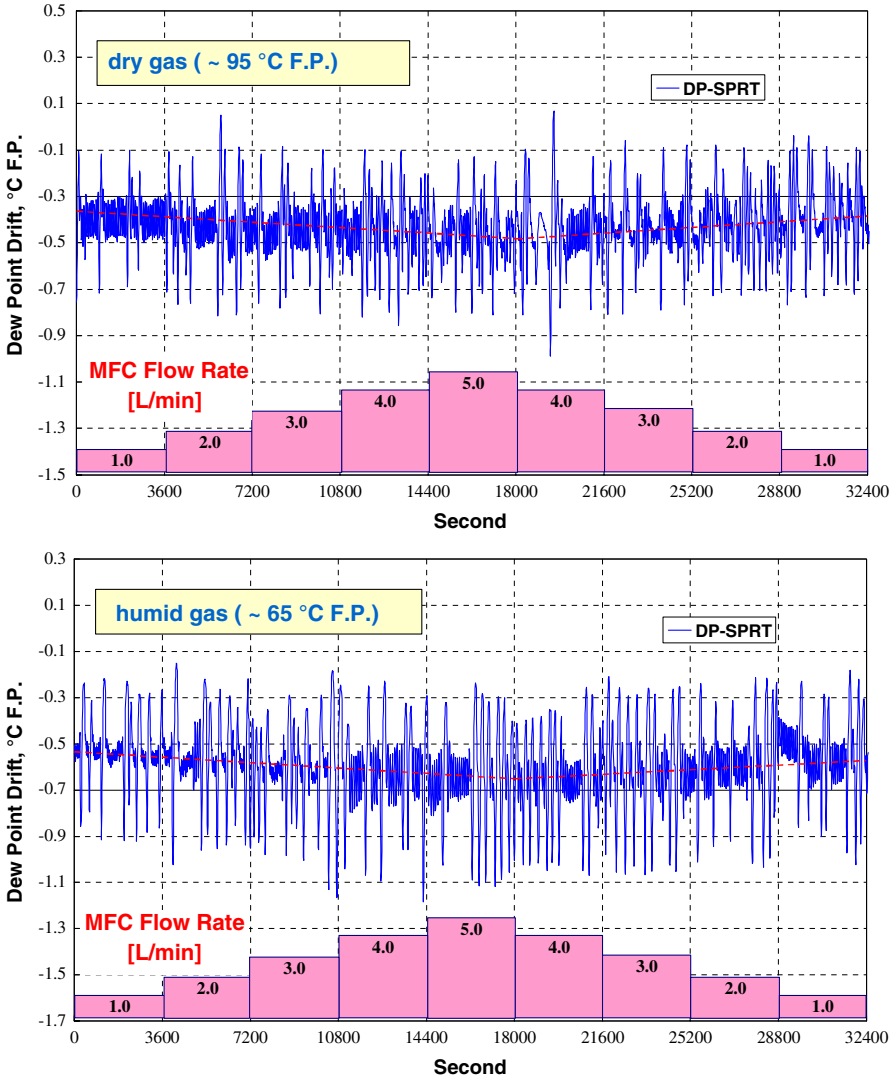

Fig. 5 Saturation capability test with gas flow rate at a saturator temperature of −70 °C

downstream end of the saturator and the hygrometer increased by only about 30 Pa, which would cause only a 0.004 °C frost-point depression.

3.3 Performance and Validation Evaluation

In Fig. 6, measurements of the frost point of the gas exiting the LFPG by an automatic dew point hygrometer (MBW DP30) are shown. The measured range for the frost-point generation (−99 °C to −40 °C) is wider than was expected at the beginning of

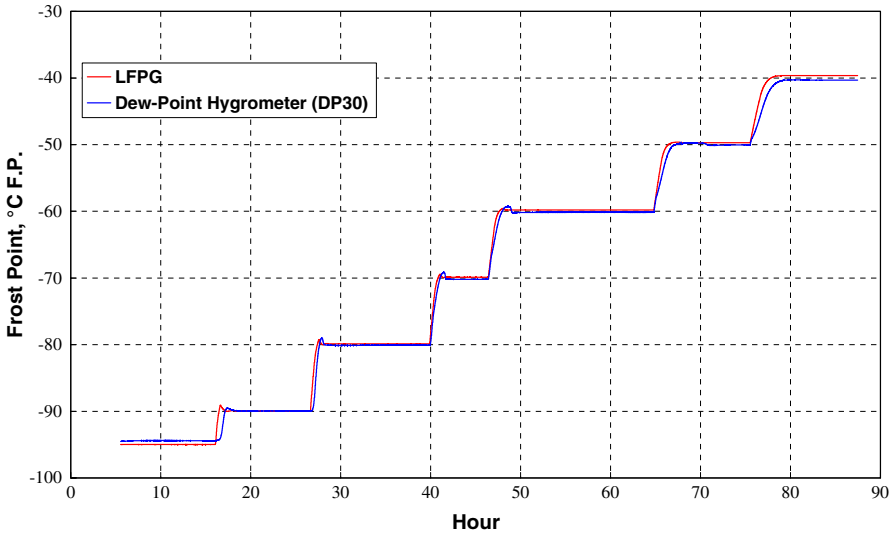

Fig. 6 Performance test of the LFPG with a dew-point hygrometer

this study (−90 °C to −60 °C). The differences between the dew-point hygrometer and the saturator temperature at frost points lower than −90 °C in the graph are not due to saturation capability, but are rather due to the limited capability of the dew-point meter in the low range.

Essentially, for the validation of a humidity generator, the gravitational method is used, but it is difficult to use this in the low frost-point range. In order to provide a validation, a two-temperature precision humidity generator, one of the national references at KRISS, is used. This has been validated from a regional intercomparison within APMP; it can produce frost points in the range (−70 to −10) °C for national calibration services, and can temporarily generate frost points as low as −80 °C. For the internal intercomparison, two dew-point hygrometers (MBW DP30 and MBW DP3-D) are employed. In Fig. 7, the comparison results are shown, and the measured differences for the frost points of the gases from two different low frost-point generators are within the uncertainties of the two dew-point hygrometers. Another method was used as a validation check. A quartz-crystal microbalance (QCM) may be used for frost-point monitoring. In Fig. 8, the frost point of the LFPG at −90.1 °C as measured by the QCM is shown. Due to the low water–vapor density, the change in the QCM signal is not large enough, but its estimated value is near a frost point of −90.6 °C. Other results are close to the one from the QCM, and within the uncertainty limits. Therefore, from a comparison of the results between the two frost-point generators via dew-point hygrometers, and a comparison between the frost point generated by the LFPG and the measured results from the QCM, one can conclude that the generated frost point of the LFPG built and tested in this study is valid.

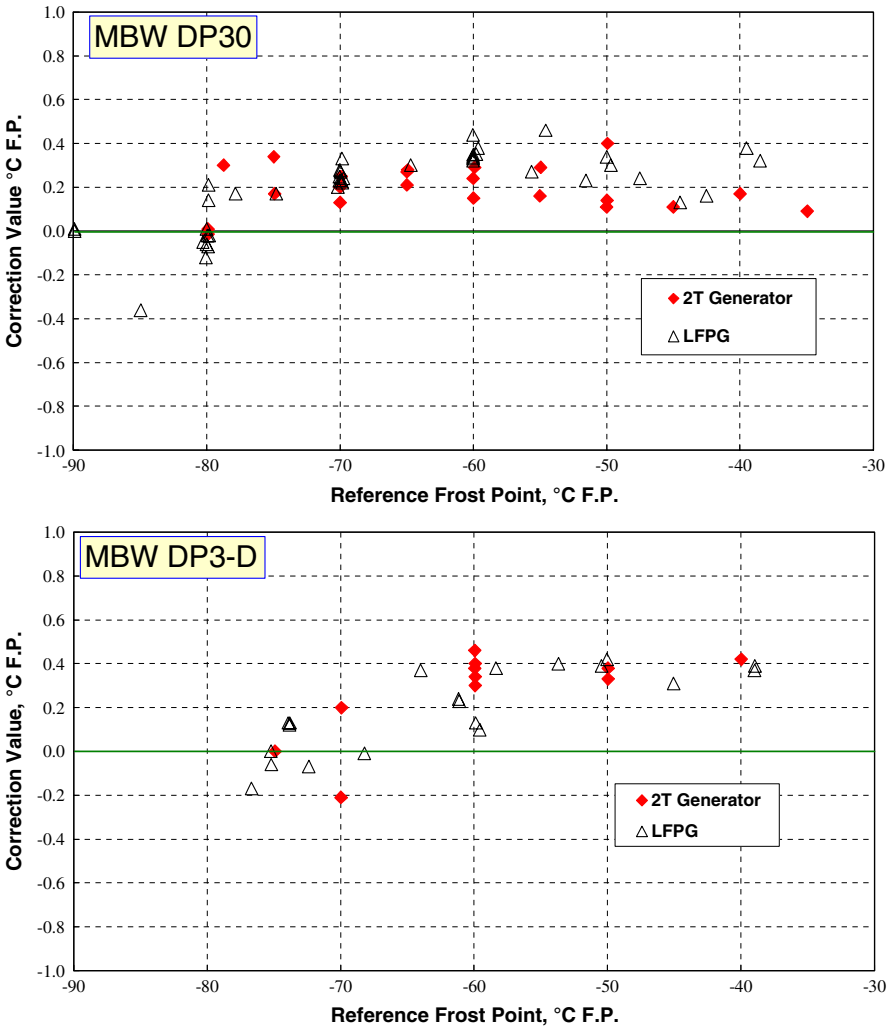

Fig. 7 Intercomparison of the measured LFPG and two-temperature humidity generator

4 Discussion

Currently, KRISS provides calibration services for the humidity range given by frost/dew points of −70 °C to +25 °C, but industries now require calibration services for humidity ranges lower than −70 °C (frost point), due to the development and technological advancement of the manufacturing industry. This study aims to satisfy such demands for the establishment of humidity standards within a new region and to increase our calibration capability. A new low frost-point generator has been developed, its performance was tested, and its validation has been accomplished. This generator employs thermal conduction from a two-stage mechanical refrigerator and

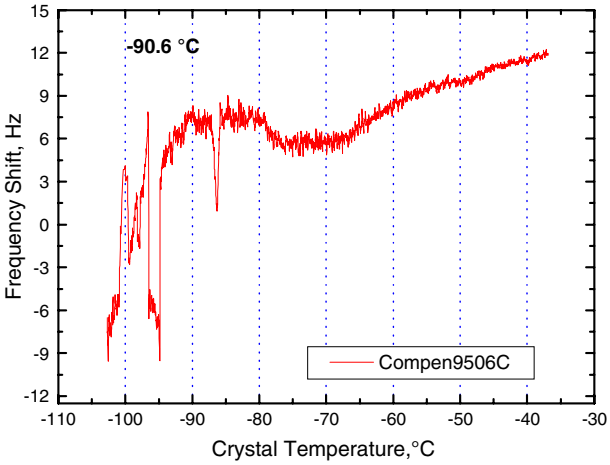

Fig. 8 Resonance frequency of a quartz resonator as a function of crystal temperature for a frost point of 90.01 °C F.P. using the LFPG

temperature control using thermoelectric-cooling devices, allowing the system to reach thermal equilibrium through solid conduction. This development has allowed KRISS to established humidity standards in the frost-point range −99 °C to −60 °C, and calibration services can be provided beginning this year. This will be very useful for calibrating chilled-mirror automatic dew-point hygrometers and thin-film humidity sensors based on alumina, in order to meet the requirements of advanced manufacturing industries, such as the semiconductor production industry.

References

1. G.E. Scace, D.C. Hovde, J.T. Hodges, P.H. Huang, J.A. Silver, J.R. Whetstone, in *Proceeedings of 3rd International Symposium on Humidity and Moisture*, vol. 1 (NPL, 1998)
2. G.E. Scace, P.H. Huang, J.T. Hodges, D.A. Olson, J.R. Whetstone, in *Proceedings of NCSL 1997 Workshop and Symposium* (Atlanta, 1997), p. 657
3. G.E. Scace, J.T. Hodges, in *Proceedings of TEMPMEKO 2001, 8th International Symposium on Temperature and Thermal Measurements in Industry and Science*, ed. by B. Fellmuth, J. Seidel, G. Scholz (VDE Verlag, Berlin, 2002), p. 597
4. D. Sonntag, Z. Meteorol. **40**, 340 (1990)
5. L. Greenspan, J. Res. NBS **80A**, 41 (1976)